

1 **Title:** MYB regulator of 'colorless' flavonols underlies the evolution of red flowers in *Lochroma*  
2 (Solanaceae)

3  
4 **Authors:** Lucas C. Wheeler<sup>1,2,†</sup>, Maximilian Larter<sup>3</sup>, Stacey D. Smith<sup>1,†</sup>

5 <sup>1</sup>Department of Ecology and Evolutionary Biology, University of Colorado, Boulder, CO, USA

6 <sup>2</sup>Department of Biology, University of South Carolina, Columbia, SC, USA

7 <sup>3</sup>National Research Institute for Agriculture, Food and Environment (INRAE), Bordeaux, France;  
8 maximilian.larter@gmail.com

9 †authors for correspondence: [lwheeler9@gmail.com](mailto:lwheeler9@gmail.com), [stacey.d.smith@colorado.edu](mailto:stacey.d.smith@colorado.edu)

10

11 **Running head:** Novel R2R3-MYB regulator of red flowers

12

13 **Keywords:** Transcriptomics, flavonoid biosynthesis, pigmentation, flower color, pelargonidin,  
14 gene regulation

15

16

17 **Abstract**

18

19 Anthocyanins, the pigments that give rise to blue, purple, red and pink colors in many flowers  
20 and fruits, are produced by the deeply conserved flavonoid biosynthesis pathway. The  
21 regulation of this pathway is thus fundamental for species differences in color across flowering  
22 plants, and a growing body of evidence implicates MYB transcription factors as key players  
23 activating or suppressing the production of different pigments. Here we demonstrate that a  
24 lineage of R2R3 MYBs that is closely related to well-known flavonol regulators (MYB12  
25 members in subgroup 7) is the primary determinant of the shift from blue to red flowers in the  
26 genus *Lochroma*. Similar to its ortholog in *Capsicum*, this *Lochroma* MYB12-like gene controls  
27 the expression of flavonoid-3'-hydroxylase, the pathway branch point between red and blue  
28 pigments, and when down-regulated, results in redirection of flux toward red pigments. These  
29 results underscore the importance of transcription factor evolution in generating phenotypic  
30 novelty as well as the competitive nature of interactions among flavonoid pathway branches. In  
31 addition, our study demonstrates the effectiveness of RNAseq of segregating populations, in  
32 combination with other lines of evidence, for identifying novel functional variation.

33

34

35 **Article Summary**

36

37 Although red flowers have convergently evolved in many taxa across angiosperms, the role of  
38 transcription factors in this common evolutionary shift has remained unclear. This study  
39 demonstrates that a class of R2R3 MYB transcription factors previously known for their role in  
40 pepper peel antioxidants (flavonols) acts as the key player in the origin of red flowers in the  
41 closely related genus *Lochroma*. The loss of floral expression of this MYB allows pathway flux to  
42 be redirected from 'colorless' flavonols towards the exclusive production of red pelargonidin,  
43 highlighting the role of biochemical pathway trade-offs in phenotypic evolution.

44

45

## 46 **Introduction**

47

48 Phenotypic differences between species are often controlled by differences in the timing and  
49 patterns of gene expression (Kimura *et al.*, 2008, Des Marais and Rausher, 2010, Byers *et al.*,  
50 2014). These differences in gene expression can arise through a variety of mechanisms,  
51 including changes in the *cis*-regulatory regions controlling expression (i.e., promoters,  
52 enhancers), changes in the expression or function of transcription factors, or post-transcriptional  
53 regulation (e.g., gene silencing). Many authors have argued that the *cis*-regulatory mutations  
54 will be favored during evolutionary transitions due to their modular architecture, allowing for  
55 altered expression in one context without pleiotropic effects in other contexts (Wray, 2007,  
56 Prud'homme *et al.*, 2006). However, functional changes in transcription factors can have  
57 similarly narrow consequences, depending on their specificity in terms of target genes and  
58 spatio-temporal patterns of expression (Lynch and Wagner, 2008, Panchy *et al.*, 2016, Auge *et*  
59 *al.*, 2019).

60 Plant MYB transcription factors comprise a prime example of a large and diverse gene  
61 family with highly specialized functions. Whereas animal and fungal genomes house at most a  
62 few dozen MYB genes, plant genomes contain hundreds of MYBs, even in diploid species (Shiu  
63 *et al.*, 2005, Feller *et al.*, 2011, Gates *et al.*, 2016). This expansion of MYB copies in plants is  
64 coupled with a diversification of functional roles, from defense, to coloration, to morphology  
65 (Ramsay and Glover, 2005, Wu *et al.*, 2022). Closely related MYBs often share similar  
66 regulatory functions, e.g., as activators or repressors of particular sets of target genes, but vary  
67 in their expression patterns, resulting in similar phenotypic effects albeit in different tissues or  
68 developmental stages (e.g., Millar and Gubler, 2005, Stracke *et al.*, 2007). Nevertheless, with  
69 the multitude of MYBs in every plant genome, new functional roles and patterns of  
70 diversification are continuing to be discovered (Sagawa *et al.*, 2016, Gates *et al.*, 2018, Mu *et*  
71 *al.*, 2024).

72 Among the subgroups of plant MYB transcription factors, those regulating floral  
73 coloration through the production of flavonoid pigments are among the best studied. The  
74 primary MYB activators of flavonoid synthesis fall into two subgroups of R2R3 MYBs: subgroup  
75 7 (SG7) genes that regulate the 'early' genes of the pathway (e.g., CHS, F3H) and the branches  
76 leading to flavonol production (FLS), and the subgroup 6 (SG6) genes that regulate the 'late'  
77 steps of the pathway (e.g., DFR, ANS) leading to anthocyanin pigments (Dubos *et al.*, 2010,  
78 Albert *et al.*, 2014) (Figure 1). Anthocyanins give rise to the red, purple and blue floral hues,

79 while flavonols can modify these colors as co-pigments and provide UV-absorbing patterns,  
80 such as nectar guides and bullseyes (Sheehan *et al.*, 2016, Todesco *et al.*, 2022). Thus, both  
81 types of compounds (anthocyanins and flavonols) are important contributors to floral coloration  
82 and are often jointly produced in developing petals.

83 While this general early/late regulatory architecture is well-conserved across flowering  
84 plants (Mol *et al.*, 1998, Schwinn *et al.*, 2014), the factors determining the type of flavonol or  
85 anthocyanin produced appear more variable across species, and perhaps for that reason, are  
86 not as well understood. Both flavonols and anthocyanins are produced at three hydroxylation  
87 levels (mono-, di-, and tri-) that have different spectral properties, and their relative expression  
88 depends on the expression of the so-called branching enzymes, F3'H and F3'5'H (Figure 1). For  
89 example, when both enzymes are highly expressed, flowers will produce the tri-hydroxylated  
90 flavonoids, such as the blue delphinidin pigments, whereas when these enzymes are not  
91 present, flowers will produce the red pelargonidin pigments (Wessinger and Rausher, 2012;  
92 Figure 1). The F3'H enzyme, which is responsible for conversion of DHK (the precursor of the  
93 flavonol kaempferol and the red pigment pelargonidin) into DHQ (the precursor of the flavonol  
94 quercetin and the purple pigment cyanidin), appears to be regulated by subgroup 7 MYBs in  
95 *Arabidopsis* and *Capsicum* (Stracke *et al.*, 2007, Wu *et al.*, 2023) and subgroup 6 MYBs in  
96 petunia and *Antirrhinum* (Albert *et al.*, 2011, Schwinn *et al.*, 2006). The other branching enzyme,  
97 F3'5'H, has been lost in many flowering plant lineages (e.g., morning glories, mustards)  
98 (Rausher, 2006, Falginella *et al.*, 2010), but in those which have retained the encoding gene, its  
99 expression is typically co-regulated with the late genes by the subgroup 6 MYBs (Albert *et al.*,  
100 2011).

101 In the present study, we investigate the regulatory control of *F3'h* expression in  
102 *Lochroma* (nightshade family, Solanaceae), one of several genera in which red pelargonidin-  
103 producing flowers have evolved from blue delphinidin-producing ancestors. Previous work  
104 demonstrated that this flower color transition involved three genetic changes, including the floral  
105 down-regulation of *F3'h*, the evolution of substrate specificity in DFR, and the loss of the *F3'5'h*  
106 gene in the red-flowered species (Smith and Rausher, 2011, Smith *et al.*, 2013). Among these  
107 changes, the loss of *F3'h* expression has the largest effect on pigment production because it  
108 largely eliminates flux away from DHK, allowing anthocyanin production to be redirected  
109 towards pelargonidin (Smith and Rausher, 2011; Figure 1). Moreover, this shift in *F3'h*  
110 expression is due to a *trans*-regulatory mutation, as the genotype at the *F3'h* locus itself does  
111 not predict flower color in segregating populations (Smith and Rausher, 2011). This unknown

112 regulator of *F3'h*, which segregates as a single gene, was termed the 'T-locus' (Smith and  
113 Rausher, 2011).

114 Here we use a suite of genomic, transcriptomic, and biochemical approaches to identify  
115 candidates for the T-locus responsible for the shift toward pelargonidin production and in turn,  
116 the evolution of red flowers in *lochroma*. Using biochemical and expression data, we first sorted  
117 individuals from a backcross population by pigment phenotype and corresponding difference in  
118 *F3'h* expression. Next, we searched the floral transcriptomes of these two pools of individuals  
119 for genes that match the predicted allelic pattern (e.g., homozygous for the red-flowered parent  
120 allele in the pink/red-flowered pool) and show the predicted association with *F3'h* expression.  
121 Our analyses point to a single R2R3 MYB transcription factor that is related to the MYB12  
122 members of Solanaceae subgroup 7 MYBs but falls in a deeply diverged clade, only functionally  
123 characterized in chili peppers. As we discuss, these results suggest that the subgroup 7 MYBs  
124 may be much more diverse than previously known and play an underappreciated role in flower  
125 color evolution through their effects on flavonol production.

126

127

## 128 **Materials and methods**

129

### 130 **Source populations and phenotyping**

131

132 Individuals of the blue-flowered *I. cyaneum* were crossed with the red-flowered *I. gesnerioides*  
133 to create segregating populations to dissect the genetic basis of their flower color differences  
134 (Smith and Rausher, 2011). The blue-flowered state is ancestral in *lochroma* and corresponds  
135 to the production of delphinidin-derived anthocyanins, while the red-flowered derived state  
136 involves the production of pelargonidin-derived anthocyanins (Figure 1; Smith and Rausher,  
137 2011). The *I. cyaneum* parent was grown from seed from a cultivated accession from the  
138 Missouri Botanical Gardens, originally collected by W. G. D'Arcy, and the *I. gesnerioides* parent  
139 was grown from the Solanaceae Germplasm collection in the Botanical Garden of Nijmegen  
140 (accession number 944750129). Herbarium vouchers for these accessions are Smith 265 and  
141 266 (WIS), respectively. A single F1 was backcrossed to the *I. gesnerioides* parent, and  
142 progeny from the resulting backcross population were genotyped at *F3'5'h* and *Dfr* (Smith and  
143 Rausher, 2011; Table 1). Anthocyanin production was previously characterized using HPLC and  
144 revealed three pigment phenotypes (purple-flowered individuals producing primarily cyanidin,

145 pink-flowered individuals producing mostly pelargonidin, and red-flowered individuals producing  
146 almost entirely pelargonidin) (Smith and Rausher 2011). The purple-flowered individuals share  
147 high *F3'h* expression and are inferred to carry a dominant 'blue' allele at a segregating trans-  
148 acting factor (the '*T*-locus', Smith and Rausher 2011) (Table 1).

149

## 150 Biochemical phenotyping and RNA-seq of backcross individuals

151

152 We performed RNA-Seq on corolla tissue from 24 backcross individuals segregating for the  
153 putative *T*-locus. We sampled 12 individuals with each inferred *T*-locus genotype: *Tt*  
154 corresponding to one dominant 'blue' allele and high *F3'h* expression or *tt* corresponding to two  
155 recessive red alleles and low *F3'h* expression (Table 1). We divided these 12 among the  
156 possible genotypes at the other two loci that affect flower color in this cross (*Dfr* and *F3'5'h*). *Dfr*  
157 shows functional specialization, with the red allele specialized for activity on DHK (Smith *et al.*  
158 2013), while *F3'5'h* is absent from the red parent genome (Smith and Rausher, 2011). With four  
159 possible combinations at these other two loci (*Dd/F-*, *Dd/-*, *dd/F-*, *dd/-*), we sampled three  
160 biological replicates of each within the groups of 12 (Table 1). We included all possible  
161 genotypic combinations at the three loci influencing flower color in order to isolate the *T*-locus  
162 while balancing across the effects of these other loci. For RNA extraction, we flash-froze corolla  
163 tissue from buds of roughly 1.25cm in length, which is equivalent to *Petunia* bud Stage 5 (Pollak  
164 *et al.*, 1993). This developmental stage shows expression of both early and late pathway genes  
165 in the anthocyanin pathway (Larter *et al.*, 2018). Total RNA was extracted with the Spectrum  
166 Total RNA extraction kit (Sigma, St Louis, MO). Library preparation and 150-base-pair paired-  
167 end mRNA sequencing was carried out by Novogene (Sacramento, CA).

168

## 169 Identifying SNPs associated with flower color and *F3'h* expression

170

171 We used the reference genome assembly for *Lochroma cyaneum* (Powell *et al.*, 2022) to call  
172 SNP variants and filter the RNASeq dataset for candidates for the *T*-locus. RNAseq reads were  
173 aligned with STAR (Dobin *et al.*, 2013), and the resulting BAM files were used as input for  
174 bcftools mpileup with default settings to call variants. We filtered variants by base call quality,  
175 only retaining variants with quality score greater than or equal to 20. We used the resulting VCF  
176 file for subsequent analyses of associations with the color phenotype.

177 We first split the filtered VCF files into two subsets, one for all samples with purple  
178 cyanidin-producing flowers (inferred *Tt* genotype at *T*-locus) and one for those with pink or red  
179 mostly pelargonidin-producing flowers (inferred *tt* genotype at *T*-locus) (Table 1). In order to  
180 identify SNPs that differ between these two pools, we used *pyvcf* (Casbon, 2012) to filter the  
181 variants to include only those that are present in all “*Tt*” individuals and not present in any “*tt*”  
182 individuals. This strict criterion resulted in a set of SNPs that perfectly co-segregate with the  
183 high or low *F3’h* expression (see Results). Most of the SNPs are located on chromosome 5, but  
184 some mapped to smaller scaffolds that were not incorporated into the reference assembly (See  
185 Figure S1). We then used *promer* from Mummer4 (Marçais *et al.*, 2018) and D-genies  
186 (Cabanettes and Klopp, 2018) to align these scaffolds back to the *I. cyaneum* and tomato  
187 reference genomes.

188 In addition to this filtering approach, we performed a case-control GWAS with the variant  
189 calls in GEMMA (Zhou and Stephens, 2012). We set phenotypes to 0 (purple-flowered *Tt*  
190 plants) or 1 (pink/red-flowered *tt* plants) and fit a univariate linear mixed model with the full set of  
191 variants. We then plotted the location of all analyzed variants on the assembled *I. cyaneum*  
192 chromosomes and identified variants with significant phenotypic associations.

193

#### 194 Co-expression of candidate genes with *F3’h*

195

196 We predicted that if the *T*-locus is a transcriptional regulator, its expression will likely track that  
197 of *F3’h* in the segregating backcross. Thus, we used expression data from the 24  
198 transcriptomes to quantify levels of expression and test for correlations between *F3’h* and loci  
199 carrying associated SNPs (previous section). We first created a *de novo* transcriptome for the  
200 blue-flowered parent (*I. cyaneum*) to ensure that we captured all expressed genes. For this  
201 assembly, we used single-end Illumina RNA-seq data from reproductive, seed, and vegetative  
202 tissues from *I. cyaneum* from a previous study (Powell *et al.*, 2022) and assembled the  
203 transcripts using the pipeline developed in Wheeler *et al.* (2022). Briefly, we corrected read  
204 errors in the 128,433,717 raw reads using Rcorrector (Song and Florea, 2015) and removed  
205 unfixable reads using *unfixable\_filter.py* (Yang and Smith, 2014). We trimmed adaptor  
206 sequences from the filtered reads using Trimmomatic (Bolger *et al.*, 2014) and used the  
207 trimmed reads for *de novo* assembly with Trinity (Grabherr *et al.*, 2011). We removed apparent  
208 chimeric sequences using *run\_chimera\_detection.py* (Morales-Briones *et al.*, 2021), with a  
209 reference BLAST database consisting of sequences from *Arabidopsis*, *Solanum*, and *Petunia*.  
210 We then used Corset (Davidson and Oshlack, 2014) to cluster transcripts and

211 *filter\_corset\_output.py* (Yang and Smith, 2014) to remove redundant transcripts. Finally, we  
212 predicted complete CDS from the Corset-filtered transcripts using TransDecoder (Haas *et al.*,  
213 2013).

214 Next, we quantified gene expression by pseudo-aligning reads from each backcross  
215 individual to the predicted CDS in the transcriptome using Salmon (Patro *et al.*, 2017). We  
216 calculated estimated read counts and TPM for each transcript. We imported Salmon quant files,  
217 partitioned by inferred *T*-locus genotype (*Tt/tt*), into DESeq2 with *tximport* (Soneson *et al.*, 2015)  
218 and used the *DESeqDataSetFromTximport* function to create a DESeq analysis object, with  
219 treatments corresponding to the *T*-locus genotype. We quantified differential expression  
220 between these subsets using the *DESeq* function. We filtered the resulting transcripts by  
221 adjusted p-value with a significance threshold of  $\text{padj}=0.05$  to identify significant DE transcripts.

222 We used WGCNA (Langfelder and Horvath, 2008) to identify modules of co-expressed  
223 genes, as we predict that the *T*-locus would be co-expressed with *F3'h* and possibly other  
224 flavonoid biosynthesis genes. WGCNA computes pairwise correlation coefficients, which then  
225 are converted to an adjacency matrix with the raw values raised to a soft-thresholding power ( $\beta$ )  
226 to approximate a scale-free network. For our data, we selected a  $\beta$  of 7, which corresponds to  
227 an  $R^2$  value of 0.88 with the scale-free model and a mean connectivity of 20.4 (See Figure S2).  
228 We initially used blockwise module detection on the full de novo transcriptomic dataset of  
229 19,184 genes, and from this first pass, we retained modules with a correlation of 0.2 or greater  
230 with the trait of interest (color phenotype/inferred *T*-locus genotype). The filtered dataset  
231 contained 4854 genes, which allowed us to examine smaller modules (minimum size of 20  
232 genes). After hierarchical clustering, we merged modules that were 90% similar and re-  
233 calculated correlations between the module eigengenes and the trait.

234 We exported the resulting module containing *F3'h* to Cytoscape format using  
235 *exportNetworkToCytoscape* and extracted the topology overlap matrix (TOM) edge weights. We  
236 plotted the distribution of weights for edges containing *F3'h* and for all other edges and used Z-  
237 scores to capture how extreme each co-expression relationship is within the context of the  
238 module. We considered genes that emerged from the association mapping (above) and  
239 presented significantly correlated expression with *F3'h* as strong candidates for the *T*-locus.

240

## 241 Phylogenetic analysis of *MYB12-like* genes and other SG7 MYBs

242

243 Our combined analyses of SNP association and gene expression strongly implicated an R2R3  
244 MYB, which we refer to as *lochroma cyaneum MYB12-like* following the nomenclature in

245 *Capsicum* (see Results). As R2R3 MYBs comprise a large group of functionally distinct  
246 transcription factors, we carried out phylogenetic analysis to identify the most closely related  
247 copies in other model Solanaceae and in *Arabidopsis*. We used BLAST searches to retrieve the  
248 top hits from tomato, potato, groundcherry, chilipepper, *Nicotiana benthamiana*, and *Arabidopsis*  
249 *thaliana* and created a protein alignment with MAFFT v. 7 (Kato and Standley, 2013) using  
250 default settings. As BLAST results suggested that the most similar sequences belonged to the  
251 flavonoid-regulating subgroup 7 (SG7) MYBs, we included the R2 and R3 MYB domains  
252 through to the SG7 motif (Stracke *et al.*, 2007, Stracke *et al.*, 2001) in the alignment. The  
253 downstream positions were trimmed as they were hypervariable and could not be confidently  
254 aligned. We estimated a maximum-likelihood phylogeny using this SG7 amino acid alignment  
255 with the best-fitting model of amino acid substitutions (Q.plant+G4) and 1000 bootstrap  
256 replicates in IQ-TREE 2.3.6 (Nguyen *et al.*, 2015, Minh *et al.*, 2020). We rooted the resulting  
257 topology on the lineage leading to the clade containing AtMYB111, AtMYB11 and AtMYB12  
258 (Schilbert and Glover, 2022).

259         Based on this broader phylogenetic analysis, we identified a set of MYBs most closely  
260 related to the candidate locus. We next estimated a tree from full length coding sequences  
261 (CDS) from those closely related copies, which are more easily aligned. We included six  
262 additional *Lochrominae* sequences assembled by mapping reads from floral bud transcriptome  
263 data onto the *Lochroma cyaneum* genome sequence, again using STAR. Each of these six  
264 species is represented by two biological replicates; a consensus of the two was used for the  
265 phylogeny and the replicates were used to estimate the levels of MYB12-like expression in each  
266 species using Salmon as above. We estimated the maximum likelihood tree from the CDS  
267 alignment with IQ-TREE, using the best-fitting model of nucleotide substitutions (TIM3+F+G4).

268

269

## 270 **Results**

271

### 272 Localization of associated SNPs with flower color in the *Lochroma* genome

273

274 We recovered 92 SNPs that perfectly co-segregate with the two phenotypic pools, i.e.,  
275 distinguish purple-flowered *Tt* and pink/red-flowered *tt* pools). The majority of these SNPs (49,  
276 53%) fall on chromosome 5 of the *L. cyaneum* reference assembly. We also found 28 SNPs  
277 mapping to a roughly 620 Kb scaffold (00085) and the remainder (15) mapping to three

278 additional unincorporated scaffolds (See Figure S1). Our subsequent analyses suggest that  
279 these scaffolds represent segments of chromosome 5 that were not included during the  
280 assembly process (Powell *et al.*, 2022). For example, scaffold00085 aligns well with tomato  
281 chromosome 5 (See Figure S3), and 95% of the CDS retrieved from that scaffold have top hits  
282 on tomato chromosome 5. This region appears nested within the larger region of *I. cyaneum*  
283 chromosome 5 where most of the SNP associations are clustered (Figure 2). The three smaller  
284 scaffolds with associated SNPs (See Figure S1) also BLAST to tomato chromosome 5 and were  
285 also likely excluded during assembly. Thus, all SNPs recovered from the co-segregation  
286 analysis appear to be localized along a small region of *I. cyaneum* chromosome 5.

287 We carried out a case-control GWAS using the same set of variant calls. This analysis  
288 similarly retrieved associations exclusively on chromosome 5, with significant hits in the gene-  
289 dense region in the last 500kb of the chromosome (Figure 2; See Figure S4). This region of the  
290 genome contains 468 gene models (See Table S1), 352 of which are functionally annotated in  
291 the genome (See Table S2). Twenty-eight of these genes are annotated as transcription factors  
292 and only one corresponds to a known group of flavonoid regulators. This locus (IC05g034110)  
293 is annotated as a MYB111 transcription factor based on similarity with AtMYB111, a flavonol-  
294 regulating subgroup 7 MYB (Stracke *et al.*, 2007); we will refer to this gene as *lochroma*  
295 *cyaneum MYB12-like (IcMYB12-like)* based on the phylogenetic analysis (see below). The  
296 region also contains copies of one of the upstream pathway enzymes, chalcone synthase  
297 (CHS), as well as UDP-glycosyltransferase (UGT), which can glycosylate various flavonoids.

298

## 299 Patterns of differential expression and co-expression

300

301 Our DEseq2 analysis identified 58 significantly differentially expressed transcripts between the  
302 two phenotypic pools in our backcross (See Table S3). The MYB transcription factor *IcMYB12-*  
303 *like* appears as the sixth most strongly differentially expressed gene between the pools ( $\log_2$ -  
304 fold change = -6.35, or ca. 82-fold lower expression in the pink/red pool). Its putative target,  
305 *F3'h*, is the eighth most differentially expressed ( $\log_2$ -fold change = -5.83, or ca. 57-fold lower  
306 expression in the pink/red pool). Note that the expression of *F3'h* in many of these individuals  
307 was previously measured with qPCR (Table 1; Smith and Rausher, 2011); this analysis confirms  
308 the strength and degree of the differential expression between individuals presenting the  
309 alternate pigment phenotypes (Figure 3A). A similar degree of differential expression was found  
310 for *FIs* between the two pools, and three other flavonoid pathway genes (*Chs*, *UGt*, and *3Gt*)

311 also appear among the list of significantly DE genes (See Table S3). These patterns could  
312 indicate some degree of regulatory control of *LcMYB12-like* over other pathway steps.

313 In addition to examining DE genes between the two phenotypic pools, we explored co-  
314 expression of genes across the entire set of 24 backcross individuals. If *LcMYB12-like* indeed  
315 activates floral *F3'h* expression, we expect the two genes to show correlated expression and to  
316 belong to the same co-expressed module of genes. Consistent with this prediction, our WGCNA  
317 analysis recovered a module of 52 genes containing *F3'h* and *LcMYB12-like* (See Table S4).  
318 Out of the 34 modules found in the analysis, the module is the only one significantly correlated  
319 with the pigment phenotype (purple vs. pink/red,  $R^2=-0.92$ ,  $p=1e^{-10}$ , See Figure S5). Within this  
320 module, *LcMYB12-like* is tightly co-expressed with *F3'h* (Figure 3B, See Table. S4). The  
321 connectivity between *F3'h* and *LcMYB12-like*, measured as topological overlap matrix (TOM)  
322 values from the WGCNA analysis, was the second highest in the set of all edges involving *F3'h*  
323 (Z-score: 1.96) with only the edge connecting *F3'h* and *Fls* having a higher value (Z-score: 2.56)  
324 (See Fig S6). We also found a tight connection between *LcMYB12-like* and *Fls* (Z-score: 1.83),  
325 suggesting that both *F3'h* and *Fls* are both regulated by *LcMYB12-like*. Four other flavonoid  
326 pathway genes, *Chs*, *Chi*, *3Gt*, and *Ugt* appear in the module associated with the phenotype,  
327 and all except for *Chi* are directly connected to *LcMYB12-like* (See Table S4; Figure 3B). Eight  
328 other loci within phenotype-associated module are connected to *LcMYB12-like* (e.g., DETOX-35-  
329 like-2 and the F-box protein At5g07610-like), although no functional connection is known. Three  
330 of the genes connected to *LcMYB12-like* (R1A-10, the F-box protein At5g07610-like and UGT)  
331 fall in the same genomic region as *LcMYB12-like* (See Table S2), suggesting that these co-  
332 expression patterns may be related to co-localization within the genome (Michalak, 2008).  
333 Indeed, differentially expressed transcripts are clustered around *LcMYB12-like* (See Figure S7).  
334 Nevertheless, both *F3'h* and *Fls* occur outside of the region containing *LcMYB12-like* (Figure 2),  
335 excluding co-localization as an explanation for their strong co-expression with *LcMYB12-like*.

336

### 337 Phylogenetic relationship of *LcMYB12-like* to other MYB transcription factors

338

339 We used BLAST searches to retrieve similar sequences to *LcMYB12-like*. The top hits from  
340 Arabidopsis and Solanaceae genomes corresponded to members of subgroup 7 of R2R3 MYB  
341 transcription factors (Stracke *et al.*, 2001). This subgroup controls flavonol production in  
342 Arabidopsis (Stracke *et al.*, 2007) by regulating upstream steps such as CHS, CHI, and FLS, as  
343 well as the glycosyltransferases that stabilize these products. Maximum-likelihood analysis  
344 revealed that *LcMYB12-like* and highly similar sequences from pepper and potato are closely

345 related to subgroup 7 but fall in a separate subclade, with strong support (Figure 4A). Subgroup  
346 7 MYBs have been well characterized in Solanaceae (e.g., Ballester *et al.*, 2010, Song *et al.*,  
347 2019) and appear functionally similar to their orthologs in *Arabidopsis*. *lochroma* possesses an  
348 SG7 MYB that is closely related to these well-characterized MYB12 genes (IC05g030210,  
349 Figure 4A) in addition to the divergent sequence (IC05g034110), which we refer to as a *MYB12-*  
350 *like* gene following the naming of *CaMYB12-like* in *Capsicum* (CA05g18430 in Figure 4A).

351 Using additional BLAST searches beyond nightshade crops, we identified an additional  
352 member of the *MYB12-like* clade in *Lycium*, which we used to root the phylogeny including the  
353 additional lochrominae sequences (Figure 4B). The topology is similar to the species tree  
354 (Deanna *et al.*, 2019) although most of the branches are unsupported given that the sequences  
355 present few differences (See Figure S8). Examining the expression of *MYB12-like* in these taxa  
356 in relation to their floral flavonol production (Larter *et al.*, 2019), we observed that species with  
357 higher *MYB12-like* expression also produce higher amounts of flavonols (Figure 4B), which are  
358 mainly quercetin glycosides (Berardi *et al.*, 2016). This pattern aligns well with the proposed  
359 function of *MYB12-like* in activating *F3'h*, which in turn produces DHQ, the precursor of  
360 quercetin (Figure 1)

361

## 362 Discussion

363

364 This study aimed to identify the gene underlying the so-called *T*-locus, which acts as a  
365 transcriptional regulator of *F3'h* to determine flower color in the nightshade genus *lochroma*. By  
366 carrying out RNASeq of floral bud tissue from multiple backcross individuals with *T*-locus  
367 genotypes assigned based on flower color (Figure 1B), we pinpointed an R2R3 MYB  
368 transcription factor as the strongest candidate for the *T*-locus. First, our SNP-association studies  
369 narrowed the candidate region to 10Mb near the end of chromosome 5 (Figure 2; See Figure  
370 S4). This region of the genome contains 468 gene models, including 28 annotated as  
371 transcription factors. Among these, only one of these corresponds to a class of genes, SG7  
372 MYBs, known to be involved in regulating flavonoid biosynthesis. This *MYB12-like* gene shows  
373 tightly correlated expression with *F3'h* across the backcross ( $r=0.91$ , Figure 3A). Indeed, these  
374 two genes emerge as part of a compact module in transcriptome-wide co-expression analyses,  
375 with *F3'h* having a stronger connection with *MYB12-like* than any other gene in the floral  
376 transcriptome with the exception of *Fls* (Figure 3B; See Figure S6). Given that the effect of the  
377 *T*-locus could be due to coding sequences changes only, this set of analyses cannot  
378 conclusively eliminate other candidate transcription factors in the associated region of the

379 genome. Nevertheless, our phylogenetic analyses identify *lcMYB12-like* as an ortholog of  
380 chillipepper *CaMYB12-like*, a recently characterized flavonoid regulator, which like its *lochroma*  
381 ortholog, acts as a positive regulator of *F3'h* (Wu *et al.*, 2023). Together, these lines of evidence  
382 argue that the *T*-locus corresponds to the *MYB12-like* gene in *lochroma*, which drives the origin  
383 of red flowers by altering floral flavonoid composition. Below we discuss how these findings  
384 contribute to our broader understanding of flower color evolution.

385

## 386 The role of MYB transcription factors in shaping floral hue

387

388 While genetic studies of flower color have long implicated subgroup 6 R2R3 MYBs as the major  
389 determinants of floral pigment intensity (e.g., Quattrocchio *et al.*, 1999, Schwinn *et al.*, 2006,  
390 Streisfeld *et al.*, 2013), work on the genetic basis of changes in floral hue has implicated a wide  
391 variety of molecular mechanisms (Wessinger and Rausher, 2012, Berardi *et al.*, 2021,  
392 Quattrocchio *et al.*, 2006). Differences in the type of anthocyanins produced, which in turn  
393 influence the type of flower color, can arise from shifts in gene regulation (either in *cis*- or *trans*-)  
394 as well as changes in the function of pathway enzymes (Hopkins and Rausher, 2011,  
395 Wessinger and Rausher, 2015, Smith and Rausher, 2011, Smith *et al.*, 2013, Wheeler *et al.*,  
396 2023). Nevertheless, the identity of transcription factors that influence the type of anthocyanin  
397 produced (as opposed to the overall amount) has remained nebulous.

398         Because of the shared precursors within the flavonoid pathway, subgroup 7 (SG7)  
399 transcriptional regulators of flavonol production can directly influence anthocyanin production,  
400 and, as shown in the present study, the type of anthocyanin produced as well. The deeply  
401 conserved structure of the pathway presents multiple branching points where a single precursor  
402 can be converted in different products depending on the enzymes present and their properties  
403 (Tohge *et al.*, 2013, Winkel-Shirley, 2001). The colorful anthocyanins share dihydroflavonol  
404 precursors (DHK, DHQ, DHM) with flavonols, creating the potential for competition between  
405 DFR and FLS for these substrates (Figure 1A). Thus, the upregulation of SG7 MYBs and, in  
406 turn, their targets (*Chs*, *Chi*, *F3h*, *F3'h*, *Fls* and sometimes *F3'h*) generally reduces anthocyanin  
407 production in favor of flavonols to produce paler flowers (Holton *et al.*, 1993, Yuan *et al.*, 2016,  
408 Wheeler *et al.*, 2023). The precise effect of altering the expression of SG7 MYBs on flower color  
409 will, however, depend on their target genes and the substrate preferences of multifunctional  
410 pathway enzymes (e.g., DFR, FLS).

411         In the case of *lochroma*, the ability of the SG7 *MYB12-like* gene to alter flower color is  
412 likely due to the combination of a narrowing of target genes and strong substrate preferences

413 among downstream enzymes. While the pepper *CaMYB12-like* gene activates a broad suite of  
414 early genes (*Chs*, *Chi*, *F3h*, *F3'h*, *Fls*, *3GT*, Wu *et al.*, 2023), the *lochroma* ortholog only shows  
415 strong co-expression with *F3'h* and *Fls* (plus weaker co-expression with *Chs*, *3Gt* and, *Ugt*),  
416 indicating a reduced suite of targets. The broad upstream action by *CaMYB12-like* is similar to  
417 that of the other well-known SG7 MYBs in Solanaceae (*SIMYB12* in tomato, Ballester *et al.*,  
418 2010, Fernandez-Moreno *et al.*, 2016; *NtMYB12* in tobacco, Song *et al.*, 2019), suggesting that  
419 coordinated regulation of 'early' genes represents the ancestral state and that the functional  
420 shift toward specificity has occurred along the *MYB12-like* lineage leading to *lochroma*.  
421 Accordingly, the loss of *MYB12-like* expression in *I. gesnerioides* flowers is not associated with  
422 a complete disruption in floral flavonoid pigment production (Berardi *et al.*, 2021, Larter *et al.*,  
423 2019), but a targeted reduction in DHQ through lower *F3'h* expression. The resulting  
424 accumulation of DHK is not converted to kaempferol, likely because of coordinated loss of *Fls*  
425 expression and its low preference for DHQ, at least in the berry-fruited Solanaceae like  
426 *lochroma* (Bovy *et al.*, 2007, Berardi *et al.*, 2016, Rosa-Martínez *et al.*, 2023). Instead, this DHK  
427 precursor is converted to red pelargonidin pigments by the DFR enzyme, which in *I.*  
428 *gesnerioides*, is specialized for DHK (Smith *et al.*, 2013). Smith *et al.* (2013) hypothesized that,  
429 during the evolutionary transition from blue to red flowers, the *trans*-regulatory loss of *F3'h*  
430 expression occurred first, allowing the flux to shift toward red pigmentation. Under this scenario,  
431 the selection would be expected to favor increased activity of DFR on DHK to allow efficient  
432 conversion to red pelargonidins.

433 This *MYB12-like*-mediated biochemical trade of blue anthocyanins plus flavonols for red  
434 anthocyanins alone may have also carried ecological consequences for relationships with  
435 pollinators. In addition to acting as co-pigments, flavonols increase floral UV-absorbance, which  
436 is attractive to moth pollinators (Sheehan *et al.*, 2016), and can also enhance fly and bee  
437 visitation if associated with floral patterning (Koski and Ashman, 2014). Indeed, insects  
438 comprise only 10% of pollinator visits to *lochroma gesnerioides* compared hummingbirds, which  
439 account for 90% of visits (Smith *et al.*, 2008). This lack of UV-absorbing flavonols is isolated to *I.*  
440 *gesnerioides* flowers as the leaves produce comparable amounts of flavonols (specifically  
441 quercetin) as the blue-flowered *I. cyanuem* (Berardi *et al.*, 2016) and the expression of *F3'h* is  
442 actually higher in *I. gesnerioides* leaves than in those of *I. cyanuem* (Smith and Rausher, 2011).  
443 The targeted effects of *MYB12-like* on floral flavonols may have thus created an accessible  
444 evolutionary pathway to red flowers, given that a loss of quercetin across the entire plant would  
445 carry significant negative pleiotropic effects (Ryan *et al.*, 2001, Singh *et al.*, 2021).

446

## 447 MYB transcription factors in the evolution of species differences

448

449 Closely related species of flowering plants are often distinguished by subtle differences in their  
450 reproductive organs, e.g., in the color, shape, scent, or pubescence of flowers or fruits. MYB  
451 transcription factors control many of these aspects of morphological development and epidermal  
452 cell fate (Ramsay and Glover, 2005, Hileman, 2014), which may help to explain their prevalence  
453 in underlying fixed differences between species (e.g., Preston *et al.*, 2011, Castillejo *et al.*,  
454 2020, Gates *et al.*, 2018, Yarahmadov *et al.*, 2020). In fact, MYB transcription factors may act  
455 as speciation genes when the phenotypic differences resulting from changes in their function or  
456 expression leads to reproductive isolation (Streisfeld *et al.*, 2013, Sheehan *et al.*, 2016, Lüthi *et al.*,  
457 2022). Through its simultaneous effects on visible anthocyanins and UV-absorbing  
458 pigments, changes in floral *MYB12-like* expression could have played a role in species  
459 divergence, although the split between the red-flowered clade containing *I. gesnerioides* and its  
460 blue-flowered relatives likely occurred 5 to 10 million years ago (Huang *et al.*, 2023), and the  
461 two lineages no longer occur in hybrid zones. The *I. arborescens* complex (the “A” clade sensu  
462 Smith and Baum (2006)) presents a stronger opportunity for dissecting the role of *MYB12-like* in  
463 floral isolation as red-flowered, low-flavonol primarily-hummingbird-pollinated species (e.g., *I.*  
464 *edule*) co-occur and hybridize with flavonol-rich insect-pollinated species (e.g., *I. arborescens*)  
465 (Smith *et al.*, 2008; Figure 4B).

466 *Cis*-regulatory mutations involving MYBs appear to be a major target for evolutionary  
467 transitions, and our results suggest that regulatory changes, as opposed to functional variation,  
468 drive the effects of *MYB12-like* on flower color in *Lochroma*. First, the *MYB12-like* sequence  
469 from *I. gesnerioides* shows 6 fixed amino acid differences from its closest blue-flowered relative  
470 (*I. calycinum*), however all but one of these variants (a threonine indel close to the 3' end, See  
471 Figure 7) are segregating across *Lochroma* species with both low and high flavonol  
472 accumulation (Figure 4B). Moreover, *MYB12-like* expression levels are strongly predictive of  
473 pathway activity. Within the backcross, the red *I. gesnerioides* parent allele of *MYB12-like* is  
474 expressed at extremely low levels, which in homozygous state translates to a near absence of  
475 *F3'h* expression (Figure 3A). This relationship extends above the species level, where lower  
476 levels of *MYB12-like* expression appear to be associated with lower levels of quercetin flavonols  
477 (Figure 4B). Beyond *Lochroma*, *cis*-regulatory mutations at MYB transcription factors frequently  
478 contribute to within and among species differences in flower color (Martins *et al.*, 2017,  
479 Streisfeld *et al.*, 2013, Fattorini and Ó'Maoiléidigh, 2022), a pattern that has been attributed to  
480 their comparatively limited pleiotropic effects (Sobel and Streisfeld, 2013). Nevertheless, the

481 precise changes in the MYB promoters are unknown in these natural systems. Identifying the  
482 causal mutation(s) will require fine dissection of the promoter region along with *in vivo* or *in vitro*  
483 assays of various constructs (e.g., Espley *et al.*, 2009, Jia *et al.*, 2021). Although transformation  
484 remains challenging outside of model systems, pinpointing these causal variants is important for  
485 ultimately understanding how and why MYBs and the modules they control can be deployed in  
486 new developmental contexts.

487

## 488 **Conclusions**

489

490 As a powerful group of antioxidants, flavonols have long been the focus of efforts in plant  
491 breeding, resulting in a detailed understanding of the subgroup 7 MYBs that largely control their  
492 expression across flowering plants. Within the nightshades, the best known of these MYBs are  
493 the orthologs of MYB12, which contribute to stress tolerance in tobacco (Song *et al.*, 2019) and  
494 the color of the fruit peel in tomato (Ballester *et al.*, 2010) via their effects on flavonoid  
495 production. This gene family is also expressed in Solanaceae flowers (Zheng *et al.*, 2021),  
496 activating early branches of the pathway to provide both flavonol co-pigments and the  
497 substrates for anthocyanin biosynthesis. Our work reveals that, in addition to this canonical  
498 'MYB12' group of SG7 MYBs, *Ipomoea* flowers also express a more divergent 'MYB12-like'  
499 lineage that has evolved narrow specificity for FLS and F3'H. This specialization, together with  
500 flower-specific expression, allows *IcMYB12-like* to act as the switch between blue and red  
501 flowers. Piecing together the origin of this gene's role in floral flavonoid production will require  
502 additional sampling of closely related genomes as they emerge. Still, our study together with the  
503 larger body of literature underscores how the diversification of MYB transcription factors is  
504 intimately connected to novel plant phenotypes, from intraspecific polymorphisms to  
505 interspecific differences.

506

507

508

## 509 **Data Availability Statement**

510 RNA-seq data from the backcross individuals have been uploaded to the SRA under Bioproject  
511 PRJNA1092111. Data for the other six species have been uploaded to SRA Bioproject  
512 PRJNA1102413. Code and additional data used in the analyses are available at

513 <https://osf.io/j5m8f/>.

514

515 **Acknowledgements**

516 The authors thank Adrian Powell (Boyce Thompson Institute) for providing access to the  
517 *lochroma cyaneum* genome through the SolGenomics website.

518

519 **Funding**

520 This work was supported by the National Science Foundation [grant number 1553114 to  
521 S.D.S.]. The RMACC Summit and Alpine supercomputers used for the computational work are  
522 also supported by the National Science Foundation [grant numbers ACI-1532235, ACI-1532236,  
523 and ACI 2201538].

524

525 **Conflict of Interest**

526 No conflict of interest declared.

527

528

## References

- Albert NW, Davies KM, Lewis DH, Zhang H, Montefiori M, Brendolise C, Boase MR, Ngo H, Jameson PE, Schwinn KE. 2014. A conserved network of transcriptional activators and repressors regulates anthocyanin pigmentation in eudicots. *Plant Cell*, 26: 962-980.
- Albert NW, Lewis DH, Zhang H, Schwinn KE, Jameson PE, Davies KM. 2011. Members of an R2R3-MYB transcription factor family in *Petunia* are developmentally and environmentally regulated to control complex floral and vegetative pigmentation patterning. *Plant Journal*, 65: 771-84.
- Auge GA, Penfield S, Donohue K. 2019. Pleiotropy in developmental regulation by flowering-pathway genes: is it an evolutionary constraint? *New Phytologist*, 224: 55-70.
- Ballester AR, Molthoff J, de Vos R, Hekkert B, Orzaez D, Fernández-Moreno JP, Tripodi P, Grandillo S, Martin C, Heldens J, Ykema M, Granell A, Bovy A. 2010. Biochemical and molecular analysis of pink tomatoes: deregulated expression of the gene encoding transcription factor SIMYB12 leads to pink tomato fruit color. *Plant Physiology*, 152: 71-84.
- Berardi AE, Esfeld K, Jäggi L, Mandel T, Cannarozzi GM, Kuhlemeier C. 2021. Complex evolution of novel red floral color in *Petunia*. *Plant Cell*, 33: 2273-2295.
- Berardi AE, Hildreth SB, Helm RF, Winkel BS, Smith SD. 2016. Evolutionary correlations in flavonoid production across flowers and leaves in the lochrominae (Solanaceae). *Phytochemistry*, 130: 119-27.
- Bolger AM, Lohse M, Usadel B. 2014. Trimmomatic: a flexible trimmer for Illumina sequence data. *Bioinformatics*, 30: 2114-20.
- Bovy A, Schijlen E, Hall RD. 2007. Metabolic engineering of flavonoids in tomato (*Solanum lycopersicum*): the potential for metabolomics. *Metabolomics*, 3: 399-412.
- Byers KJ, Vela JP, Peng F, Riffell JA, Bradshaw HD. 2014. Floral volatile alleles can contribute to pollinator-mediated reproductive isolation in monkeyflowers (*Mimulus*). *Plant Journal*, 80: 1031-1042.
- Cabanettes F, Klopp C. 2018. D-GENIES: dot plot large genomes in an interactive, efficient and simple way. *PeerJ*, 6: e4958.
- Casbon J. 2012. PyVCF - A Variant Call Format Parser for Python v. 0.3.0. 0.3.0 ed. <https://github.com/jamescasbon/PyVCF>.

- Castillejo C, Waurich V, Wagner H, Ramos R, Oiza N, Muñoz P, Triviño JC, Caruana J, Liu Z, Cobo N, Hardigan MA, Knapp SJ, Vallarino JG, Osorio S, Martín-Pizarro C, Posé D, Toivainen T, Hytönen T, Oh Y, Barbey CR, Whitaker VM, Lee S, Olbricht K, Sánchez-Sevilla JF, Amaya I. 2020. Allelic variation of MYB10 is the major force controlling natural variation in skin and flesh color in Strawberry (*Fragaria* spp.) fruit. *The Plant Cell*, 32: 3723-3749.
- Davidson NM, Oshlack A. 2014. Corset: enabling differential gene expression analysis for de novo assembled transcriptomes. *Genome Biology*, 15: 410.
- Deanna R, Larter MD, Barboza GE, Smith SD. 2019. Repeated evolution of a morphological novelty: a phylogenetic analysis of the inflated fruiting calyx in the Physalideae tribe (Solanaceae). *American Journal of Botany*, 106: 270-279.
- Deanna R, González Ramírez I, Särkinen T, Knapp S, Sauquet H, Smith SD. Late Cretaceous origins for major nightshade lineages from total evidence timetree analysis. Invited submission for Special Issue on 'Milestones and trends: the role of the fossil record in reconstructing plant evolution' in *Annals of Botany*.
- Des Marais DL, Rausher MD. 2010. Parallel evolution at multiple levels in the origin of hummingbird pollinated flowers in *Ipomoea*. *Evolution*, 64: 2044-2054.
- Dobin A, Davis CA, Schlesinger F, Drenkow J, Zaleski C, Jha S, Batut P, Chaisson M, Gingeras TR. 2013. STAR: ultrafast universal RNA-seq aligner. *Bioinformatics*, 29: 15-21.
- Dubos C, Stracke R, Grotewold E, Weisshaar B, Martin C, Lepiniec L. 2010. MYB transcription factors in *Arabidopsis*. *Trends in Plant Science*, 15: 573-581.
- Espley RV, Brendolise C, Chagné D, Kuttly-Amma S, Green S, Volz R, Putterill J, Schouten HJ, Gardiner SE, Hellens RP, Allan AC. 2009. Multiple repeats of a promoter segment causes transcription factor autoregulation in red apples. *Plant Cell*, 21: 168-183.
- Falginella L, Castellarin SD, Testolin R, Gambetta GA, Morgante M, Di Gaspero G. 2010. Expansion and subfunctionalisation of flavonoid 3',5'-hydroxylases in the grapevine lineage. *BMC Genomics*, 11: 562.
- Fattorini R, Ó'Maoiléidigh DS. 2022. Cis-regulatory variation expands the colour palette of the Brassicaceae. *Journal of Experimental Botany*, 73: 6511-6515.
- Feller A, Machemer K, Braun EL, Grotewold E. 2011. Evolutionary and comparative analysis of MYB and bHLH plant transcription factors. *Plant J*, 66: 94-116.
- Fernandez-Moreno JP, Tzfadia O, Forment J, Presa S, Rogachev I, Meir S, Orzaez D, Aharoni A, Granell A. 2016. Characterization of a new pink-fruited tomato mutant results in the

- identification of a null allele of the SIMYB12 transcription factor. *Plant Physiology*, 171: 1821-1836.
- Gates DJ, Olson BJSC, Clemente TE, Smith SD. 2018. A novel R3 MYB transcriptional repressor associated with the loss of floral pigmentation in *Lochroma*. *New Phytologist*, 217: 1346-1356.
- Gates DJ, Strickler SR, Mueller LA, Olson BJ, Smith SD. 2016. Diversification of R2R3-MYB transcription factors in the tomato family Solanaceae. *Journal of Molecular Evolution*, 83: 26-37.
- Grabherr MG, Haas BJ, Yassour M, Levin JZ, Thompson DA, Amit I, Adiconis X, Fan L, Raychowdhury R, Zeng Q, Chen Z, Mauceli E, Hacohen N, Gnirke A, Rhind N, di Palma F, Birren BW, Nusbaum C, Lindblad-Toh K, Friedman N, Regev A. 2011. Full-length transcriptome assembly from RNA-Seq data without a reference genome. *Nature Biotechnology*, 29: 644-52.
- Haas BJ, Papanicolaou A, Yassour M, Grabherr M, Blood PD, Bowden J, Couger MB, Eccles D, Li B, Lieber M, MacManes MD, Ott M, Orvis J, Pochet N, Strozzi F, Weeks N, Westerman R, William T, Dewey CN, Henschel R, LeDuc RD, Friedman N, Regev A. 2013. De novo transcript sequence reconstruction from RNA-seq using the Trinity platform for reference generation and analysis. *Nature Protocols*, 8: 1494-1512.
- Hileman LC. 2014. Trends in flower symmetry evolution revealed through phylogenetic and developmental genetic advances. *Philosophical Transactions of the Royal Society B*, 369.
- Holton TA, Brugliera F, Tanaka Y. 1993. Cloning and expression of flavonol synthase from *Petunia hybrida*. *Plant Journal*, 4: 1003-1010.
- Hopkins R, Rausher MD. 2011. Identification of two genes causing reinforcement in the Texas wildflower *Phlox drummondii*. *Nature*, 469: 411-4.
- Huang J, Xu W, Zhai J, Hu Y, Guo J, Zhang C, Zhao Y, Zhang L, Martine C, Ma H, Huang C-H. 2023. Nuclear phylogeny and insights into whole-genome duplications and reproductive development of Solanaceae plants. *Plant Communications*, 4: 100595.
- Jia D, Wu P, Shen F, Li W, Zheng X, Wang Y, Yuan Y, Zhang X, Han Z. 2021. Genetic variation in the promoter of an R2R3-MYB transcription factor determines fruit malate content in apple (*Malus domestica* Borkh.). *Plant Physiology*, 186: 549-568.
- Katoh K, Standley DM. 2013. MAFFT multiple sequence alignment software version 7: improvements in performance and usability. *Molecular Biology and Evolution*, 30: 772-80.

- Kimura S, Koenig D, Kang J, Yoong FY, Sinha N. 2008. Natural variation in leaf morphology results from mutation of a novel KNOX gene. *Current Biology*, 18: 672-677.
- Koski MH, Ashman T-L. 2014. Dissecting pollinator responses to a ubiquitous ultraviolet floral pattern in the wild. *Functional Ecology*, 28: 868-877.
- Langfelder P, Horvath S. 2008. WGCNA: an R package for weighted correlation network analysis. *BMC Bioinformatics*, 9: 559.
- Larter M, Dunbar-Wallis A, Berardi AE, Smith SD. 2018. Convergent evolution at the pathway Level: predictable regulatory changes during flower color transitions. *Molecular Biology and Evolution*, 35: 2159-2169.
- Larter M, Dunbar-Wallis A, Berardi AE, Smith SD. 2019. Developmental control of convergent floral pigmentation across evolutionary timescales. *Developmental Dynamics*, 248: 1091-1100.
- Lynch VJ, Wagner GP. 2008. Resurrecting the role of transcription factor change in developmental evolution. *Evolution*, 62: 2131-2154.
- Lüthi MN, Berardi AE, Mandel T, Freitas LB, Kuhlemeier C. 2022. Single gene mutation in a plant MYB transcription factor causes a major shift in pollinator preference. *Current Biology*, 32: 5295-5308.e5.
- Martins TR, Jiang P, Rausher MD. 2017. How petals change their spots: cis-regulatory re-wiring in *Clarkia* (Onagraceae). *New Phytologist*, 216: 510-518.
- Marçais G, Delcher AL, Phillippy AM, Coston R, Salzberg SL, Zimin A. 2018. MUMmer4: A fast and versatile genome alignment system. *PLoS Computational Biology*, 14: e1005944.
- Michalak P. 2008. Coexpression, coregulation, and cofunctionality of neighboring genes in eukaryotic genomes. *Genomics*, 91: 243-248.
- Millar AA, Gubler F. 2005. The *Arabidopsis* GAMYB-like genes, MYB33 and MYB65, are microRNA-regulated genes that redundantly facilitate anther development. *Plant Cell*, 17: 705-721.
- Minh BQ, Schmidt HA, Chernomor O, Schrempf D, Woodhams MD, von Haeseler A, Lanfear R. 2020. IQ-TREE 2: New models and efficient methods for phylogenetic inference in the genomic era. *Molecular Biology and Evolution*, 37: 1530-1534.
- Mol J, Grotewold E, Koes R. 1998. How genes paint flowers and seeds. *Trends in Plant Science*, 3: 212-217.
- Morales-Briones DF, Kadereit G, Tefarikis DT, Moore MJ, Smith SA, Brockington SF, Timoneda A, Yim WC, Cushman JC, Yang Y. 2021. Disentangling sources of gene tree

- discordance in phylogenomic data sets: testing ancient hybridizations in Amaranthaceae s.l. *Systematic Biology*, 70: 219-235.
- Mu Q, Wei J, Longest HK, Liu H, Char SN, Hinrichsen JT, Tibbs-Cortes LE, Schoenbaum GR, Yang B, Li X, Yu J. 2024. A MYB transcription factor underlying plant height in sorghum qHT7.1 and maize Brachytic 1 loci. *Plant Journal*, 120: 2172-2192.
- Nguyen LT, Schmidt HA, von Haeseler A, Minh BQ. 2015. IQ-TREE: a fast and effective stochastic algorithm for estimating maximum-likelihood phylogenies. *Molecular Biology and Evolution*, 32: 268-274.
- Panchy N, Lehti-Shiu M, Shiu SH. 2016. Evolution of gene duplication in plants. *Plant Physiol*, 171: 2294-2316.
- Patro R, Duggal G, Love MI, Irizarry RA, Kingsford C. 2017. Salmon provides fast and bias-aware quantification of transcript expression. *Nature Methods*, 14: 417-419.
- Pollak PE, Vogt T, Mo Y, Taylor LP. 1993. Chalcone synthase and flavonol accumulation in stigmas and anthers of *Petunia hybrida*. *Plant Physiology*, 102: 925-932.
- Powell AF, Zhang J, Hauser D, Vilela JA, Hu A, Gates DJ, Mueller LA, Li FW, Strickler SR, Smith SD. 2022. Genome sequence for the blue-flowered Andean shrub *Lochroma cyaneum* reveals extensive discordance across the berry clade of Solanaceae. *Plant Genome*, 15: e20223.
- Preston JC, Martinez CC, Hileman LC. 2011. Gradual disintegration of the floral symmetry gene network is implicated in the evolution of a wind-pollination syndrome. *Proceedings of the National Academy of Sciences USA*, 108: 2343-8.
- Prud'homme B, Gompel N, Rokas A, Kassner VA, Williams TM, Yeh SD, True JR, Carroll SB. 2006. Repeated morphological evolution through cis-regulatory changes in a pleiotropic gene. *Nature*, 440: 1050-1053.
- Quattrocchio F, Verweij W, Kroon A, Spelt C, Mol J, Koes R. 2006. PH4 of *Petunia* is an R2R3 MYB protein that activates vacuolar acidification through interactions with basic-helix-loop-helix transcription factors of the anthocyanin pathway. *Plant Cell*, 18: 1274-1291.
- Quattrocchio F, Wing J, van der Woude K, Souer E, de Vetten N, Mol J, Koes R. 1999. Molecular analysis of the anthocyanin2 gene of petunia and its role in the evolution of flower color. *Plant Cell*, 11: 1433-44.
- Ramsay NA, Glover BJ. 2005. MYB-bHLH-WD40 protein complex and the evolution of cellular diversity. *Trends Plant Sci*, 10: 63-70.
- Rausher MD. 2006. The evolution of flavonoids and their genes. In: Grotewold E, ed. *The science of flavonoids*. New York, NY: Springer New York.

- Rosa-Martínez E, Bovy A, Plazas M, Tikunov Y, Prohens J, Pereira-Dias L. 2023. Genetics and breeding of phenolic content in tomato, eggplant and pepper fruits. *Frontiers in Plant Science*, 14: 1135237.
- Ryan KG, Swinny EE, Winefield C, Markham KR. 2001. Flavonoids and UV photoprotection in *Arabidopsis* mutants. *Zeitschrift für Naturforschung - Section C Journal of Biosciences*, 56: 745-754.
- Sagawa JM, Stanley LE, LaFountain AM, Frank HA, Liu C, Yuan YW. 2016. An R2R3-MYB transcription factor regulates carotenoid pigmentation in *Mimulus lewisii* flowers. *New Phytologist*, 209: 1049-1057.
- Schilbert HM, Glover BJ. 2022. Analysis of flavonol regulator evolution in the Brassicaceae reveals MYB12, MYB111 and MYB21 duplications and MYB11 and MYB24 gene loss. *BMC Genomics*, 23: 604.
- Schwinn K, Venail J, Shang Y, Mackay S, Alm V, Butelli E, Oyama R, Bailey P, Davies K, Martin C. 2006. A small family of MYB-regulatory genes controls floral pigmentation intensity and patterning in the genus *Antirrhinum*. *Plant Cell*, 18: 831-851.
- Schwinn KE, Boase MR, Bradley JM, Lewis DH, Deroles SC, Martin CR, Davies KM. 2014. MYB and bHLH transcription factor transgenes increase anthocyanin pigmentation in petunia and lisianthus plants, and the petunia phenotypes are strongly enhanced under field conditions. *Frontiers in Plant Science*, 5: 603.
- Sheehan H, Moser M, Klahre U, Efeld K, Dell'Olivo A, Mandel T, Metzger S, Vandenbussche M, Freitas L, Kuhlemeier C. 2016. MYB-FL controls gain and loss of floral UV absorbance, a key trait affecting pollinator preference and reproductive isolation. *Nature Genetics*, 48: 159-166.
- Shiu SH, Shih MC, Li WH. 2005. Transcription factor families have much higher expansion rates in plants than in animals. *Plant Physiology*, 139: 18-26.
- Singh P, Arif Y, Bajguz A, Hayat S. 2021. The role of quercetin in plants. *Plant Physiology and Biochemistry*, 166: 10-19.
- Smith SD, Baum DA. 2006. Phylogenetics of the florally diverse Andean clade *Lochrominae* (Solanaceae). *American Journal of Botany*, 93: 1140-53.
- Smith SD, Hall SJ, Izquierdo PR, Baum DA. 2008. Comparative pollination biology of sympatric and allopatric Andean *Lochroma* (Solanaceae). *Annals of the Missouri Botanical Garden*, 95: 600-617.
- Smith SD, Rausher MD. 2011. Gene loss and parallel evolution contribute to species difference in flower color. *Molecular Biology and Evolution*, 28: 2799-2810.

- Smith SD, Wang S, Rausher MD. 2013. Functional evolution of an anthocyanin pathway enzyme during a flower color transition. *Molecular Biology and Evolution*, 30: 602-612.
- Sobel JM, Streisfeld MA. 2013. Flower color as a model system for studies of plant evo-devo. *Frontiers in Plant Science*, 4: 321.
- Soneson C, Love MI, Robinson MD. 2015. Differential analyses for RNA-seq: transcript-level estimates improve gene-level inferences. *F1000Research*, 4: 1521.
- Song L, Florea L. 2015. Rcorrector: efficient and accurate error correction for Illumina RNA-seq reads. *Gigascience*, 4: 48.
- Song Z, Luo Y, Wang W, Fan N, Wang D, Yang C, Jia H. 2019. NtMYB12 positively regulates flavonol biosynthesis and enhances tolerance to low Pi stress in *Nicotiana tabacum*. *Frontiers in Plant Science*, 10: 1683.
- Stracke R, Ishihara H, Hupé G, Barsch A, Mehrrens F, Niehaus K, Weisshaar B. 2007. Differential regulation of closely related R2R3-MYB transcription factors controls flavonol accumulation in different parts of the *Arabidopsis thaliana* seedling. *Plant J*, 50: 660-77.
- Stracke R, Werber M, Weisshaar B. 2001. The R2R3-MYB gene family in *Arabidopsis thaliana*. *Current Opinion in Plant Biology*, 4: 447-456.
- Streisfeld MA, Young WN, Sobel JM. 2013. Divergent selection drives genetic differentiation in an R2R3-MYB transcription factor that contributes to incipient speciation in *Mimulus aurantiacus*. *PLoS Genet*, 9: e1003385.
- Todesco M, Bercovich N, Kim A, Imerovski I, Owens GL, Dorado Ruiz Ó, Holalu SV, Madilao LL, Jahani M, Légaré JS, Blackman BK, Rieseberg LH. 2022. Genetic basis and dual adaptive role of floral pigmentation in sunflowers. *Elife*, 11.
- Tohge T, Watanabe M, Hoefgen R, Fernie AR. 2013. The evolution of phenylpropanoid metabolism in the green lineage. *Critical Reviews in Biochemistry and Molecular Biology*, 48: 123-152.
- Wessinger CA, Rausher MD. 2012. Lessons from flower colour evolution on targets of selection. *Journal of Experimental Botany*, 63: 5741-5749.
- Wessinger CA, Rausher MD. 2015. Ecological transition predictably associated with gene degeneration. *Molecular Biology and Evolution*, 32: 347-354.
- Wheeler LC, Dunbar-Wallis A, Schutz K, Smith SD. 2023. Evolutionary walks through flower colour space driven by gene expression in *Petunia* and allies (Petunieae). *Proceedings of the Royal Society B*, 290: 20230275.
- Winkel-Shirley B. 2001. Flavonoid biosynthesis. A colorful model for genetics, biochemistry, cell biology, and biotechnology. *Plant Physiology*, 126: 485-493.

- Wray GA. 2007. The evolutionary significance of cis-regulatory mutations. *Nat Rev Genet*, 8: 206-16.
- Wu Y, Popovsky-Sarid S, Tikunov Y, Borovsky Y, Baruch K, Visser RGF, Paran I, Bovy A. 2023. CaMYB12-like underlies a major QTL for flavonoid content in pepper (*Capsicum annuum*) fruit. *New Phytologist*, 237: 2255-2267.
- Wu Y, Wen J, Xia Y, Zhang L, Du H. 2022. Evolution and functional diversification of R2R3-MYB transcription factors in plants. *Horticulture Research*, 9: uhac058.
- Yang Y, Smith SA. 2014. Orthology inference in nonmodel organisms using transcriptomes and low-coverage genomes: improving accuracy and matrix occupancy for phylogenomics. *Molecular Biology and Evolution*, 31: 3081-3092.
- Yarahmadov T, Robinson S, Hanemian M, Pulver V, Kuhlemeier C. 2020. Identification of transcription factors controlling floral morphology in wild *Petunia* species with contrasting pollination syndromes. *Plant Journal*, 104: 289-301.
- Yuan YW, Rebocho AB, Sagawa JM, Stanley LE, Bradshaw HD. 2016. Competition between anthocyanin and flavonol biosynthesis produces spatial pattern variation of floral pigments between *Mimulus* species. *Proceedings of the National Academy of Sciences USA*, 113: 2448-2453.
- Zheng Y, Chen Y, Liu Z, Wu H, Jiao F, Xin H, Zhang L, Yang L. 2021. Important roles of key genes and transcription factors in flower color differences of *Nicotiana glauca*. *Genes (Basel)*, 12: 1976.
- Zhou X, Stephens M. 2012. Genome-wide efficient mixed-model analysis for association studies. *Nature Genetics*, 44: 821-824.

**Table 1.** Phenotypes and genotypes of sampled individuals from backcross population. The DEL, CYAN and PEL columns show the proportion of anthocyanins derived from blue delphinidin, purple cyanidin and red pelargonidin pigments, respectively (data from Smith and Rausher 2011). The expression of *F3'h* was quantified with qPCR in Smith and Rausher (2011); individuals with 'low' expression have 10-fold lower expression than those with 'high'. Individuals with high *F3'h* expression and/or primarily cyanidin production are predicted to be heterozygous at the *T*-locus with one 'blue' and one 'red' allele (*Tt*). The samples are split between *Tt* and *tt* individuals at the *T*-locus, and there are three replicates for each combination of genotypes at the other involved loci (*F3'5'h* and *Dfr*). Note that the red parental species is missing the functional copy of *F3'5'h*, so the red allele is indicated with a -.

Indiv	DEL	CYAN	PEL	<i>F3'h</i> expression	Inferred T-locus genotype	<i>F3'5'h</i>	<i>Dfr</i>
GCG22	0.2	0.68	0.1	high	<b><i>Tt</i></b>	<b><i>F-</i></b>	<i>dd</i>
GCG55	0.3	0.63	0.1	high	<b><i>Tt</i></b>	<b><i>F-</i></b>	<i>dd</i>
GCG11	0.24	0.61	0.15	high	<b><i>Tt</i></b>	<b><i>F-</i></b>	<i>dd</i>
GCG98	0.2	0.7	0.1	high	<b><i>Tt</i></b>	-	<b><i>Dd</i></b>
GCG84	0.03	0.67	0.30	high	<b><i>Tt</i></b>	-	<b><i>Dd</i></b>
GCG25	0.2	0.62	0.2	high	<b><i>Tt</i></b>	-	<b><i>Dd</i></b>
GCG49	0.12	0.53	0.35	high	<b><i>Tt</i></b>	<b><i>F-</i></b>	<b><i>Dd</i></b>
GCG40	0.11	0.67	0.22	high	<b><i>Tt</i></b>	<b><i>F-</i></b>	<b><i>Dd</i></b>
GCG94	0.3	0.57	0.2	n/a	<b><i>Tt</i></b>	<b><i>F-</i></b>	<b><i>Dd</i></b>
GCG60	0.01	0.70	0.29	high	<b><i>Tt</i></b>	-	<i>dd</i>
GCG18	0.01	0.84	0.14	high	<b><i>Tt</i></b>	-	<i>dd</i>
GCG76	0.05	0.81	0.14	n/a	<b><i>Tt</i></b>	-	<i>dd</i>
GCG2	0.24	0.07	0.69	low	<i>tt</i>	<b><i>F-</i></b>	<b><i>Dd</i></b>
GCG61	0.2	0.14	0.7	low	<i>tt</i>	<b><i>F-</i></b>	<b><i>Dd</i></b>
GCG23	0.21	0.11	0.67	low	<i>tt</i>	<b><i>F-</i></b>	<b><i>Dd</i></b>
GCG24	0.2	0.14	0.7	low	<i>tt</i>	<b><i>F-</i></b>	<i>dd</i>
GCG73	0.2	0.12	0.7	low	<i>tt</i>	<b><i>F-</i></b>	<i>dd</i>
GCG7	0.17	0.14	0.69	low	<i>tt</i>	<b><i>F-</i></b>	<i>dd</i>
GCG4	0.05	0.05	0.90	low	<i>tt</i>	-	<b><i>Dd</i></b>
GCG85	0.02	0.04	0.94	n/a	<i>tt</i>	-	<b><i>Dd</i></b>
GCG6	0.08	0.11	0.81	low	<i>tt</i>	-	<b><i>Dd</i></b>
GCG9	0.05	0.04	0.91	low	<i>tt</i>	-	<i>dd</i>
GCG104	0.1	0.08	0.9	low	<i>tt</i>	-	<i>dd</i>
GCG43	0.07	0.06	0.87	low	<i>tt</i>	-	<i>dd</i>

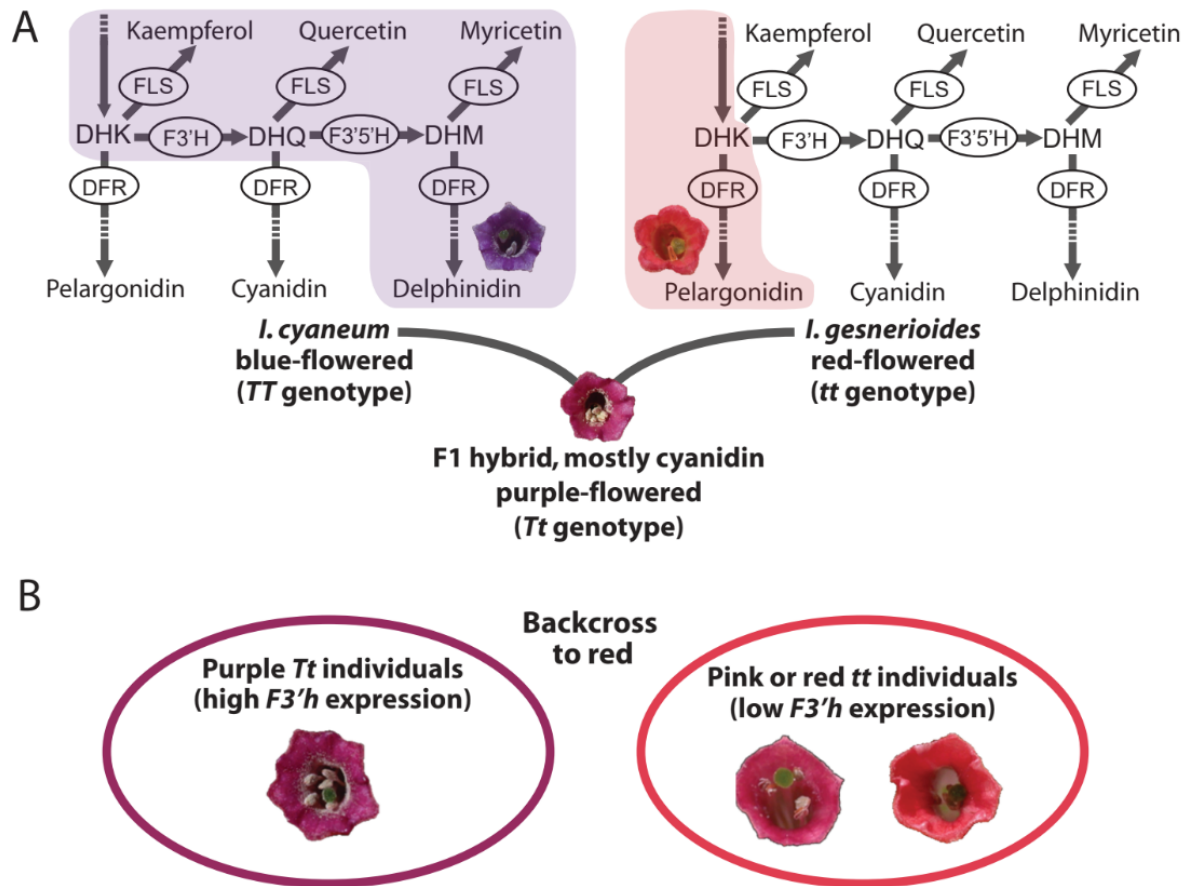


**Figure 1.** Flavonoid pigment production in parental lines and experimental design for identifying the *T*-locus. (A) Segregating backcross populations were created from parental lines of the blue-flowered *Lochroma cyaneum* and the red-flowered *I. gesnerioides*. The former makes delphinidin-derived anthocyanins and all three of flavonols (kaempferol, quercetin and myricetin) while the latter makes only pelargonidin-derived anthocyanins and kaempferol. The active branches of the pathway are shaded in each case. The enzymes shown (in ellipses) are flavonoid 3'hydroxylase (*F3'H*), flavonoid-3'5'-hydroxylase (*F3'5'H*), dihydroflavonol reductase (*DFR*) and flavonol synthase (*FLS*). Flavonoid intermediates are dihydrokaempferol (*DHK*), dihydroquercetin (*DHQ*) and dihydromyricetin (*DHM*). Additional steps upstream of *DHK* (e.g. involving chalcone synthase (*CHS*), chalcone isomerase (*CHI*) and flavanone hydroxylase (*F3H*)) and downstream of *DFR* (e.g., involving anthocyanidin synthase (*ANS*), glucosyltransferase) are not shown but indicated with the dashed portion of the arrows. Note that *F3'5'H* has 3' activity and can act on *DHK* in some taxa, but in *Lochroma*, it is specialized for *DHQ* (Smith and Rausher, 2011). The *F1* hybrid produces mainly cyanidin-derived anthocyanins and is presumed to be heterozygous at the *T*-locus, which controls *F3'h* expression. (B) Phenotypes and pools for RNASeq experiment. We divided the backcross population (*F1* crossed to the red parent) into a high *F3'h* expression purple-flowered cyanidin-producing pool (presumably *Tt*) and a low *F3'h* expression mostly or entire pelargonidin-producing pink to red-flowered pool (presumably *tt*). See Table 1 for more information on sequenced individuals.

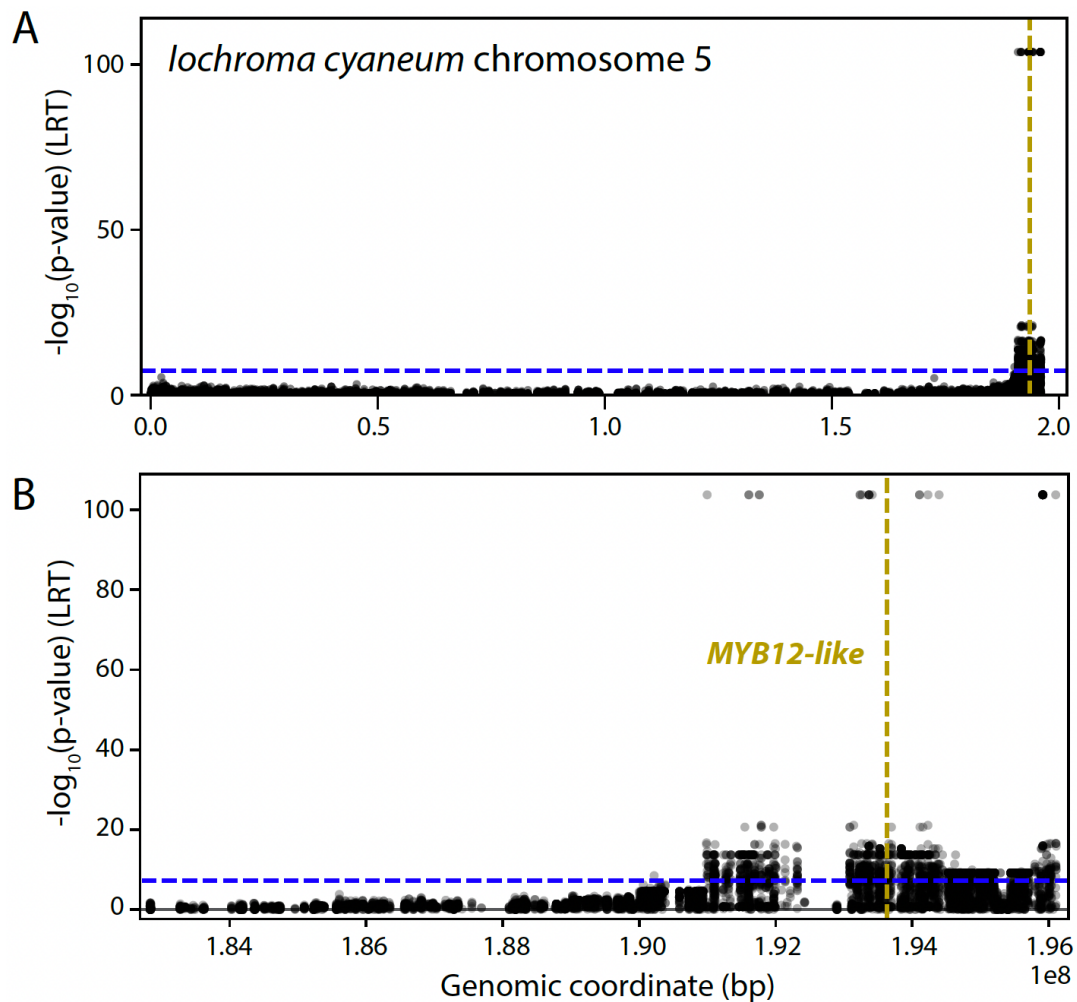


**Figure 2.** Manhattan plot showing significant SNP associations on *lochroma cyaneum* chromosome 5. The blue-dashed line marks the cutoff for genome-wide significance ( $P < 5 \times 10^{-8}$ ). The gold vertical line marks the location of the *MYB12-like* gene, which predicts *F3'h* expression. (A) The position of *MYB12-like* near the 3' prime end of the chromosome. (B) Close-up of the region containing *MYB12-like*, showing the concentration of associated SNPs in the last 500kb of the chromosome.

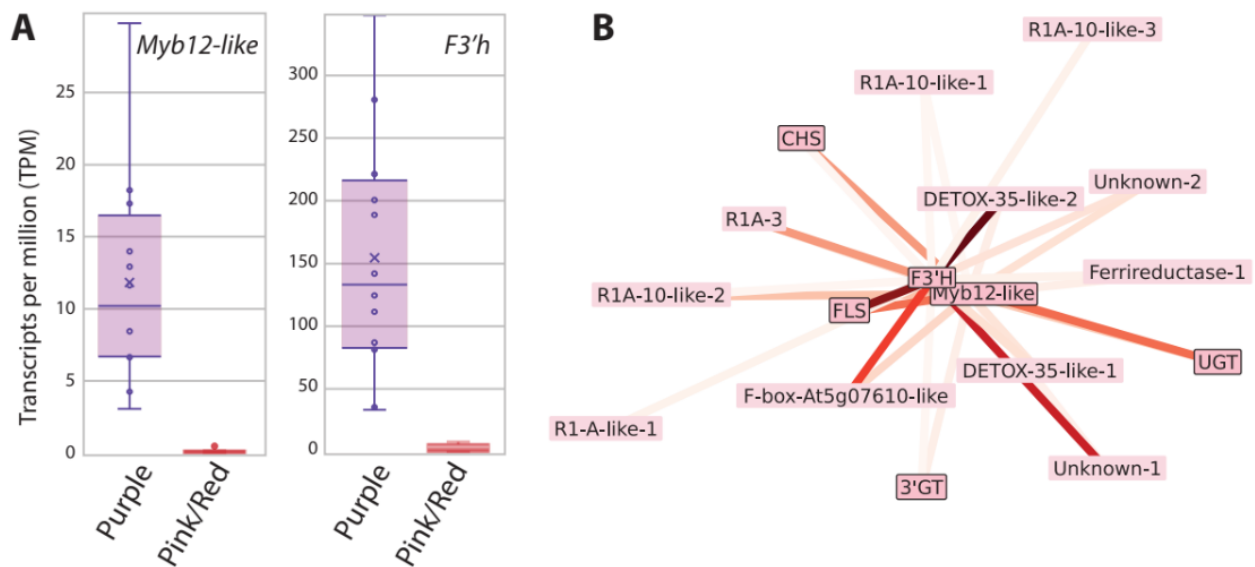


**Figure 3. Co-expression of *F3'h* and *IcMYB12-like*.** (A) Expression levels for each gene in the two phenotypic pools. Box plots mark the first and third quartiles, with a bisecting line to indicate the median. The mean is denoted with an x. The Pearson correlation coefficient for the expression of these two genes is 0.91 ( $P < 0.0001$ ). (B) Submodule from WGCNA analysis containing all edges including *F3'h* and *IcMYB12-like* (see See Table S4). The lines representing each edge are colored by the connectivity value (TOM) from WGCNA (Figure S6); more closely clustered genes are more tightly co-expressed (i.e., spring layout). Enzymes related to the flavonoid pathway (*CHS*, *FLS*, *3'GT*, *UGT*) are outlined along with *IcMYB12-like*.

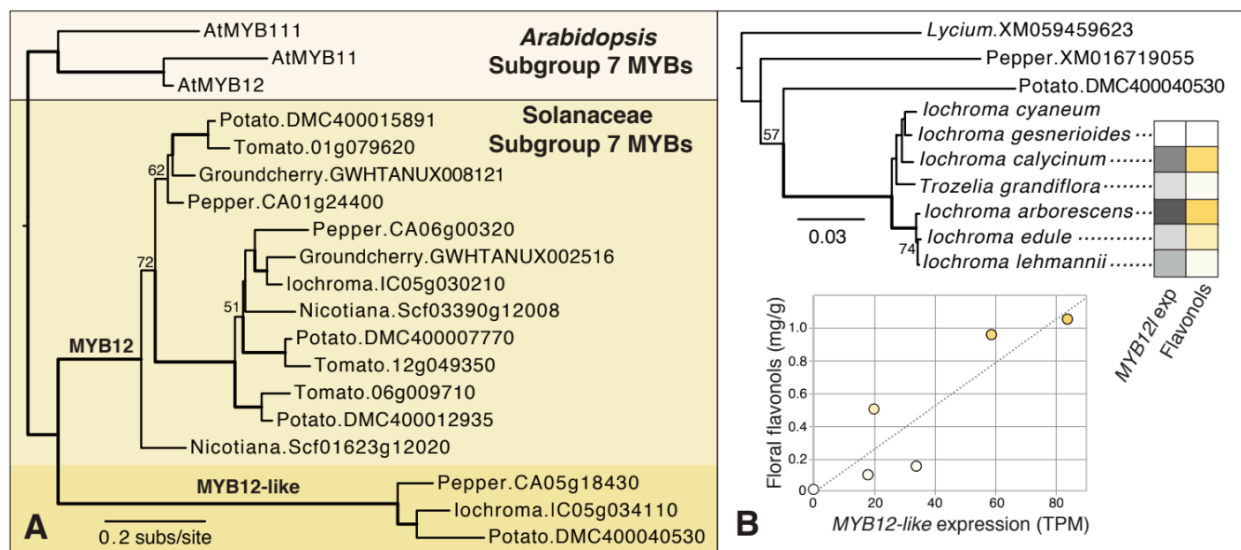


**Figure 4.** Phylogenetic position of MYB12-like proteins in relation to other subgroup 7 R2R3 MYBs. (A) Maximum likelihood phylogeny from protein sequences. Most Solanaceae subgroup 7 MYBs fall into large clade typically annotated as “MYB12”. MYB12-like sequences fall into a deeply diverged clade that appears to be sister to the MYB12 sequences. Bolded branches have >95% bootstrap support; values between 50 and 95% bootstrap support are shown. (B) Maximum likelihood phylogeny for MYB12-like sequences based on a complete CDS alignment. Bootstrap supports are shown as in (A). Tip values for *MYB12-like* expression (TPM) and floral flavonol content (in mg/g from Larter et al. 2019) for six species are colored by magnitude (see See Table S5 for raw data). These data are graphed in the inset figure with the dashed line showing the linear trend. *lochroma cyaneum* is not included as data from previous transcriptomic analyses (Gates et al. 2018) are not directly comparable with the de novo transcriptomes from the present study. Full names and sources for all sequences used in this analysis are given in See Table S6. Branch lengths in both trees are in substitutions per site.